

100 Bev correspond well to isotropic emission from a single center; the one event with energy between 100 and 1000 Bev does not have an obvious break in the angular distribution but might be explained as emission from two centers.

In considering the energy of secondary particles as a function of their angle of emission, we have examined the predictions of the two-center model under the assumption that the momentum spectrum of emitted particles is isotropic in each of the two systems. This model predicts the apparent constancy of transverse momentum, but makes the further prediction that the average transverse momentum should be lower, not only in forward and backward directions, but also around 90° in the C-system. The model also places definite restrictions on the values of energy and emis-

sion angle which the majority of the particles can have. These predictions should be susceptible to experimental test, particularly in jets with a wide separation between cones. The available experimental results from this and other published work have been studied and are seen to be readily understood in terms of the model, but are not yet sufficient to permit a definite conclusion.

ACKNOWLEDGMENTS

The author wishes to thank Professor G. Cocconi for several valuable discussions and for access to some of his private papers and some unpublished data, and Dr. R. C. Kumar who made some of the early measurements on the α-particle jet. The author is also very much indebted to Dr. E. Pickup for his continued interest and encouragement in this work.

Heavy Primary Cosmic Rays at Geomagnetic Latitude of 41°N

O. B. YOUNG AND H. Y. CHEN  
 Southern Illinois University, Carbondale, Illinois  
 (Received April 21, 1959)

This report includes the results from 9 balloon flights at geomagnetic latitude 41°N of altitude range from 70 000 to 100 000 feet. Only primaries of  $Z \geq 10$  are considered. 2410 tracks are involved, in Ilford G-5 and G-0 emulsion exposures. Given are the charge spectra, flux, mean free paths, and angular distributions.

INTRODUCTION

THIS paper represents an expansion of an investigation previously published.<sup>1</sup> The results are now based on an increase in the number of heavy nuclear

tracks from 1082 to 2021. The emulsions containing these tracks were exposed at altitudes above 90 000 feet. Also herein included are the results of an additional 389 tracks in emulsions exposed in the 67 000-foot to

TABLE I. Percent of each Z for each plate.

Nuclear charge Z	Plate number								
	HHNII	2601	4001	2588	1423	1480	37 A and B	LHNII	3200
10	21.5	26.8	20.2	16.4	19.0	29.1	18.8	24.2	36.2
11	13.6	14.2	12.0	12.6	14.2	17.1	12.4	12.8	14.7
12	16.6	18.6	19.5	11.4	13.1	12.4	16.1	15.9	8.6
13	9.5	9.1	11.6	13.9	13.6	12.4	12.2	14.7	9.1
14	8.6	6.7	5.6	11.4	7.7	10.5	10.2	9.6	9.5
15	5.3	5.2	5.6	6.3	7.1	4.2	7.5	5.1	5.6
16	2.4	2.8	3.4	1.3	1.7	1.2	2.7	3.2	3.0
17	3.9	2.8	2.2	5.0	3.0	3.5	3.0	2.5	3.9
18	2.4	1.4	2.6	5.0	2.3	2.3	2.2	0.6	2.2
19	2.4	2.8	3.0	2.5	4.1	1.6	2.5	3.2	1.3
20	2.3	1.4	2.2	5.0	2.3	0.8	3.0	1.3	2.2
21	3.1	0.7	1.9	1.3	3.0	0.4	2.7	1.8	2.2
22	1.3	1.4	3.0	1.3	4.1	1.2	2.2	1.8	0.4
23	1.7	0.7	3.0	1.3	0.6	0.4	1.7	0.6	0.4
24	2.4	2.2	2.2	2.5	1.7	0.8	1.1	1.3	0.4
25	1.2	0	0.4	1.3	0	1.6	0.3	0	0
26	1.7	1.4	1.5	1.3	1.7	0.6	1.1	1.3	0.4
No. of tracks	753	134	267	79	168	258	362	157	232
Flux, $I_0$ : multiply by $10^{-4}$ part./cm <sup>2</sup> sec sterad	2.66±0.31	2.53±0.40	2.70±0.40	2.40±0.41	2.50±0.30	2.40±0.40	2.57±0.41	2.41±0.46	2.50±0.80
Altitude (g/cm <sup>2</sup> )	9.98	17.46	7.74	11.43	15.43	15.40	7.70	32.40	52.80
Peaking angle	54°±5°	54°±5°	60°±5°	48°±5°	57°±5°	50°±5°	55°±5°	45°±5°	45°±5°

<sup>1</sup> O. B. Young and F. E. Harvey, Phys. Rev. **109**, 529 (1958).

TABLE II. Flight and plate data.

Plate	No. of tracks	Flux value, $I_0$ ( $10^{-4}$ part./cm <sup>2</sup> sec sterad)	Attenuation MFP ( $\lambda$ ) (g/cm <sup>2</sup> )	Altitude (g/cm <sup>2</sup> )	Date	Area scanned (cm <sup>2</sup> )	Time of flight (hours)	Calib. const. a	b	Thickness (microns)	Type of plate
HHNII	753	$2.66 \pm 0.31$	$21.43 \pm 0.67$	09.98	February 11, 1956	97.46	8.4	0.082	0.2	600	G-5
4001	267	$2.70 \pm 0.40$	$24.80 \pm 1.0$	07.74	June 3, 1955	21.70	9.0	0.082	0.23	600	G-5
37	362	$2.57 \pm 0.41$	$21.29 \pm 0.95$	07.70	June 3, 1955	33.44	9.3	0.06	0.18	1000	G-5
2588	79	$2.40 \pm 0.41$	24	11.43	November 18, 1954	23.45	6.2	0.065	0.2	600	G-0, G-5 200, 400
1423	168	$2.50 \pm 0.30$		15.43	May 8, 1952	32.14	7.7	0.075	0.2	600	G-5
1480	258	$2.40 \pm 0.40$		15.40	October 7, 1954	60.00	7.5	0.081	0.2	400	G-5
2601	134	$2.53 \pm 0.40$		17.41	February 5, 1954	34.70	7.0	0.057	0.2	600	G-5
LHNII	157	$2.41 \pm 0.46$	$23.39 \pm 0.91$	32.40	February 11, 1956	106.13	8.0	0.085	0.2	600	G-5
3200	232	$2.50 \pm 0.80$	24	52.80	January 24, 1955	280.0	8.0	0.072	0.2	600	G-5

Average  $I_0$  (without No. 2601) =  $2.53 \pm 0.44 \times 10^{-4}$  particles/cm<sup>2</sup> sec sterad (incomplete flight curve)  
 Average  $I_0$  (with No. 2601) =  $2.52 \pm 0.43 \times 10^{-4}$  particles/cm<sup>2</sup> sec sterad

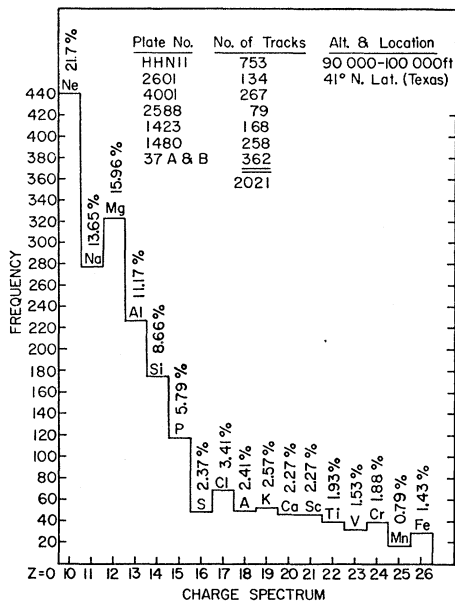


FIG. 1. Charge spectrum for 2021 tracks.

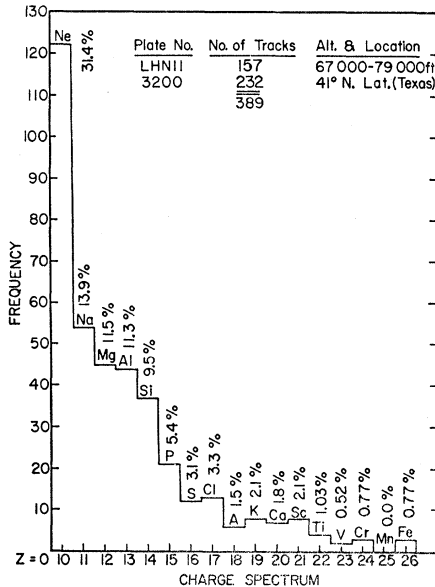


FIG. 2. Charge spectrum for 389 tracks.

73 000-foot altitude range. In the previous paper considerable attention was given to plate HHNII. One section containing 176 tracks gave results which were lower in attenuation mean free path than the figures from other plates. However, after HHNII was completely scanned, yielding 753 tracks, the results were raised from  $19 \pm 0.7$  g/cm<sup>2</sup> to  $21.43 \pm 0.67$  g/cm<sup>2</sup>.

EXPERIMENTAL METHOD

The experimental method has remained essentially unchanged. Angular distribution measurements have been added. While angles have been measured to within one degree, they are plotted more roughly, as the smaller divisions are not generally needed.

RESULTS

The results are given in Tables I and II and Figs. 1-5. Flux,  $I_0$ , has been obtained by extrapolation to the top of the atmosphere. The various values agree well, regardless of the altitudes of the balloon flights.

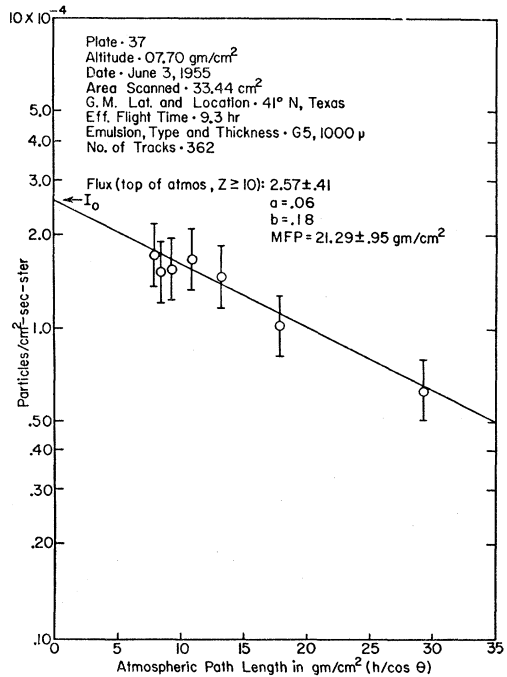


FIG. 3. Flux for plate 37.

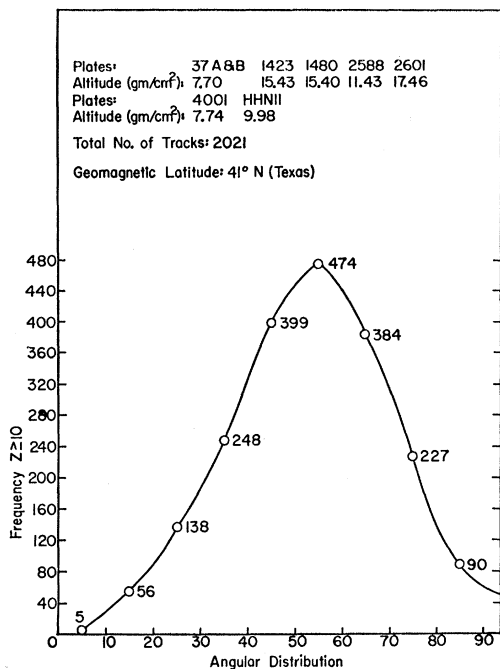


FIG. 4. Angular distribution for 2021 tracks.

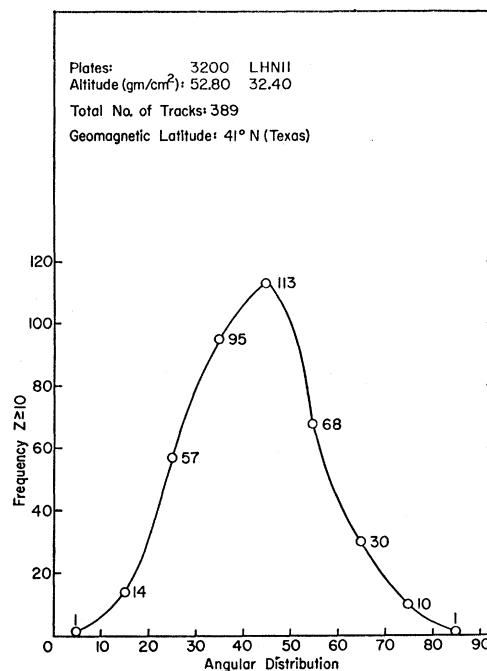


FIG. 5. Angular distribution for 389 tracks.

The charge spectrum is given for each plate in Table II. The results are combined for all plates exposed at about the same altitude in Figs. 1 and 2. For the data contained in Fig. 1 the altitudes of exposure were in the 90 000-foot to the 104 000-foot range. For the other, the altitudes were lower, being in the 67 000-foot to 79 000-foot range. The relative abundance in percent is given for each  $Z$ . However, a reader must observe that the lower the altitude of exposure, the less reliable the abundance ratios become, owing to the more rapid absorption of the heavier elements by the atmosphere and to the heavy nucleus breakups which have fragments large enough to be included among nuclei of  $Z \geq 10$ . This effect is clearly shown by comparison of the two charge spectra.

The angular distributions for each plate are given. The peaking angle, measured from the zenith, for each plate is listed in Table II. Absorption by the atmosphere

causes the peaking angle to become smaller as the altitude decreases.

The attenuation mean free path,  $\lambda$ , has been determined separately for six of the nine plates listed, with the results listed in Table I. These six values average 23.1 g/cm<sup>2</sup>. The consistency is within about 6% from the mean.

#### ACKNOWLEDGMENTS

The authors appreciate the assistance given by Marcel Schein and his Cosmic-Ray Group at the University of Chicago with whom this research was cooperatively performed. Also appreciated is the partial financial support given by the Research Corporation, by the Office of Ordnance Research of the U. S. Army, and by the International Geophysical Year Program. Thanks are also extended to the Office of Naval Research for balloon flights.